Biol. Cybern. 90, 377–389 (2004)
DOI 10.1007/s00422-004-0481-7
© Springer-Verlag 2004

Biological Cybernetics

Model of head–neck joint fast movements in the frontal plane

A. Pedrocchi, G. Ferrigno

NIT lab TBM Lab Dept. of Bioengineering, Politecnico di Milano, P.zza L. da Vinci, 32, 20133 Milan, Italy

Received: 13 May 2002 / Accepted: 1 April 2004 / Published online: 9 July 2004

Abstract. The objective of this work is to develop a model representing the physiological systems driving fast head movements in frontal plane. All the contributions occurring mechanically in the head movement are considered: damping, stiffness, physiological limit of range of motion, gravitational field, and muscular torques due to voluntary activation as well as to stretch reflex depending on fusal afferences. Model parameters are partly derived from the literature, when possible, whereas undetermined block parameters are determined by optimising the model output, fitting to real kinematics data acquired by a motion capture system in specific experimental set-ups. The optimisation for parameter identification is performed by genetic algorithms. Results show that the model represents very well fast head movements in the whole range of inclination in the frontal plane. Such a model could be proposed as a tool for transforming kinematics data on head movements in 'neural equivalent data', especially for assessing head control disease and properly planning the rehabilitation process. In addition, the use of genetic algorithms seems to fit well the problem of parameter identification, allowing for the use of a very simple experimental set-up and granting model robustness.

1 Introduction

The objective of this work is to develop a model which, taking into account anatomical and physiological considerations, is representative of fast head movement in the frontal plane. The infra-orbital line and the head position are proposed in the literature largely as variables controlled primarily by the central nervous system, since evidences of their stability in space during complex movement are known (Berthoz and Pozzo 1988; Pozzo et al. 1990, 1991; Amblard et al. 1997; Barberini and Macpherson 1998).

Correspondence to: A. Pedrocchi
(e-mail: pedrocchi@biomed.polimi.it,
Tel.: +39-2-23993346, Fax: +39-2-23993360)

The model proposed here is a complex model describing all effects occurring in head movement in the frontal plane; it is thus inherently different from a modelling approach aimed at modelling only muscle activity, but it includes all contributions, active and passive. It can be compared to a model-based plant used for neuroprostheses studies (Riener and Edrich 1999) in terms of objectives, but it is completely different in methodological approach. Indeed, in those cases complex experimental set-ups were adopted for identifying single muscle parameters, while our approach is global; parameter identification exploits a genetic algorithm approach, and experimental set-up for model identification is thus very simple.

Current knowledge in neurophysiology (Kandel et al. 1994) allows one to describe the control system of head movements in the frontal plane in response to lower segment perturbations, as reported in Fig. 1. It is assumed that neural signals concurring to the correction of the infra-orbital line alignment with the horizontal direction are linearly combined. Actually, this hypothesis is not exploited for this work and will require further investigation for future development.

The considered sensory systems monitor in a direct or indirect way the inclination of the head with respect to the horizontal (β angle in Fig. 1). Those systems' outputs are then composed to produce the alphamotoneuron activity. (s_α) are (Guitton et al. 1986):

- Proprioception, which is divided into two different blocks: H_{rp}, representing relative proprioception, depending on joint sensors, estimating head position as a result of the kinematic chain from the lower segments, and H_{ap}, the absolute proprioception, which estimates gravity direction, depending on graviceptor action.
- Vestibular system (Bronstein 1988; Pozzo et al. 1991), which is represented by two blocks: H_{sv}, static vestibular inputs from internal ear sensors, and H_{dv}, dynamic vestibular inputs from semi-circular canal action.
- Vision H_{v}.

In addition, there are two more contributions. The first is the feed-forward control (H_{ff}), representing the anticipatory postural adjustments accompanying

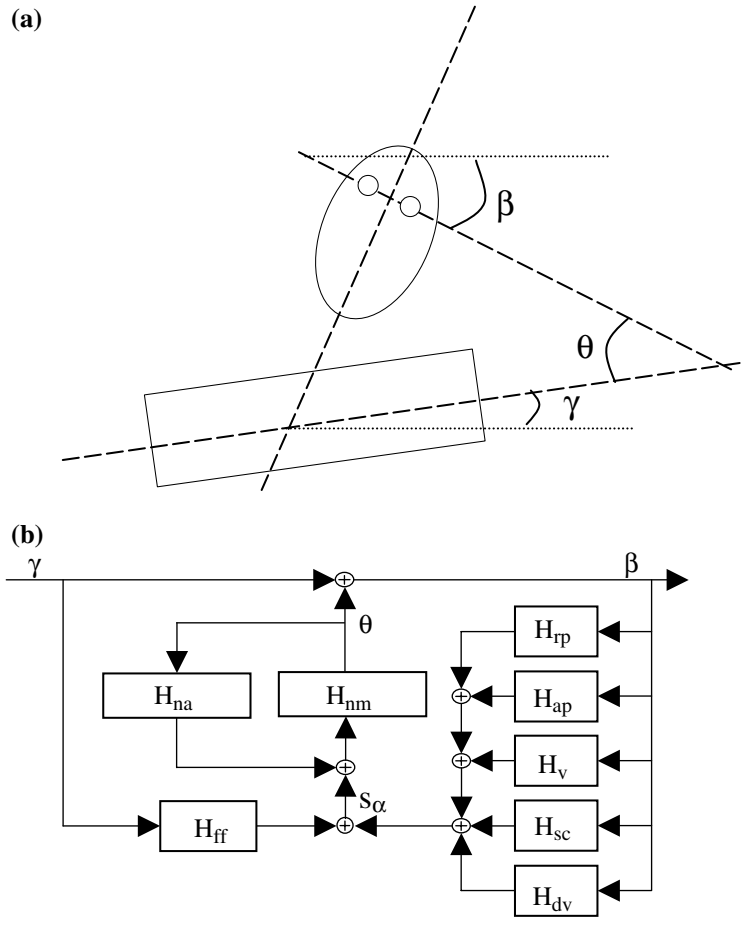

Fig. 1. **a** Definition of angles: γ is the angle between shoulders and horizontal, θ the angle between the infra-orbital line and the shoulder axis, β the angle between the infra-orbital line and the horizontal plane. **b** Systems involved in head stabilisation. H_{na} represents the neck articular sensors, H_{nm} the neuro-mechanical neck model, H_{ff} the feed-forward control system contribution, H_{rp} the relative proprioceptive systems, H_{ap} the absolute proprioceptive systems, H_v the visual system, H_{sc} the static vestibular system and H_{dv} the dynamic vestibular system contributions

voluntary movements involving shoulder axis (γ angle in Fig. 1). The latter block represents neck receptors (H_{na}), which are still part of proprioception but directly act, by spinal reflexes, on neck movement (monitoring directly θ angle in Fig. 1).

In this complex control scheme, the first aim of modelling is represented by the transfer function between the alphamotoneuron input signal s_α and head inclination. This paper describes the identification and the validation of this part of the system (H_{nm} and H_{na} in Fig. 1). It offers a tool for any further investigation aimed at defining quantitatively the "neural contribution" of each sensory system by the inverse transformation of the movement performed in the neural equivalent input.

2 Model description

The starting point for the definition of the model is the sixth-order system introduced by Zangemeister et al. (1981), which has been proposed for modelling head rotations in the coronal plane. Currently, it is still the most widely used model for such systems, and it has given rise to other muscular models.

A functional model is presented in Fig. 2, analysing the neuro-physiological and mechanical mechanisms concurring to head inclination in the frontal plane. The output variable is θ, defined as the angle between the shoulder axis and the infra-orbital line in the frontal plane (Fig. 1b). The initial conditions are that the head is perfectly vertical and still, and it is supposed that the shoulders are fixed in the horizontal position; hence in this configuration θ is equal to β (γ is zero).

As presented in Fig. 2, some mechanical contributions are to be considered in the definition of the total torque: tissue stiffness, damping and the action of gravity. Their contributions are added to the muscular torque so as to compose the total torque at the head equivalent joint.

First, we describe how those mechanical contributions are expressed in the model.

2.1 Intrinsic passive stiffness(H_{pl}, H_s)

Stiffness (Zangemeister et al. 1981) depends mainly on muscle elongation and on biological characteristics of the other tissues involved in the movement. Stiffness characteristics are represented in the model by two separate blocks:

$$H_{\text{stiffness}} = H_{\text{pl}} + H_{\text{s}} . \tag{1}$$

The first implements the physiological limit (H_{pl} block), representing the substantial effects of ligaments and joints as the inclination increases. The H_{pl} block is modelled by an exponential function of θ, with two specific parameters

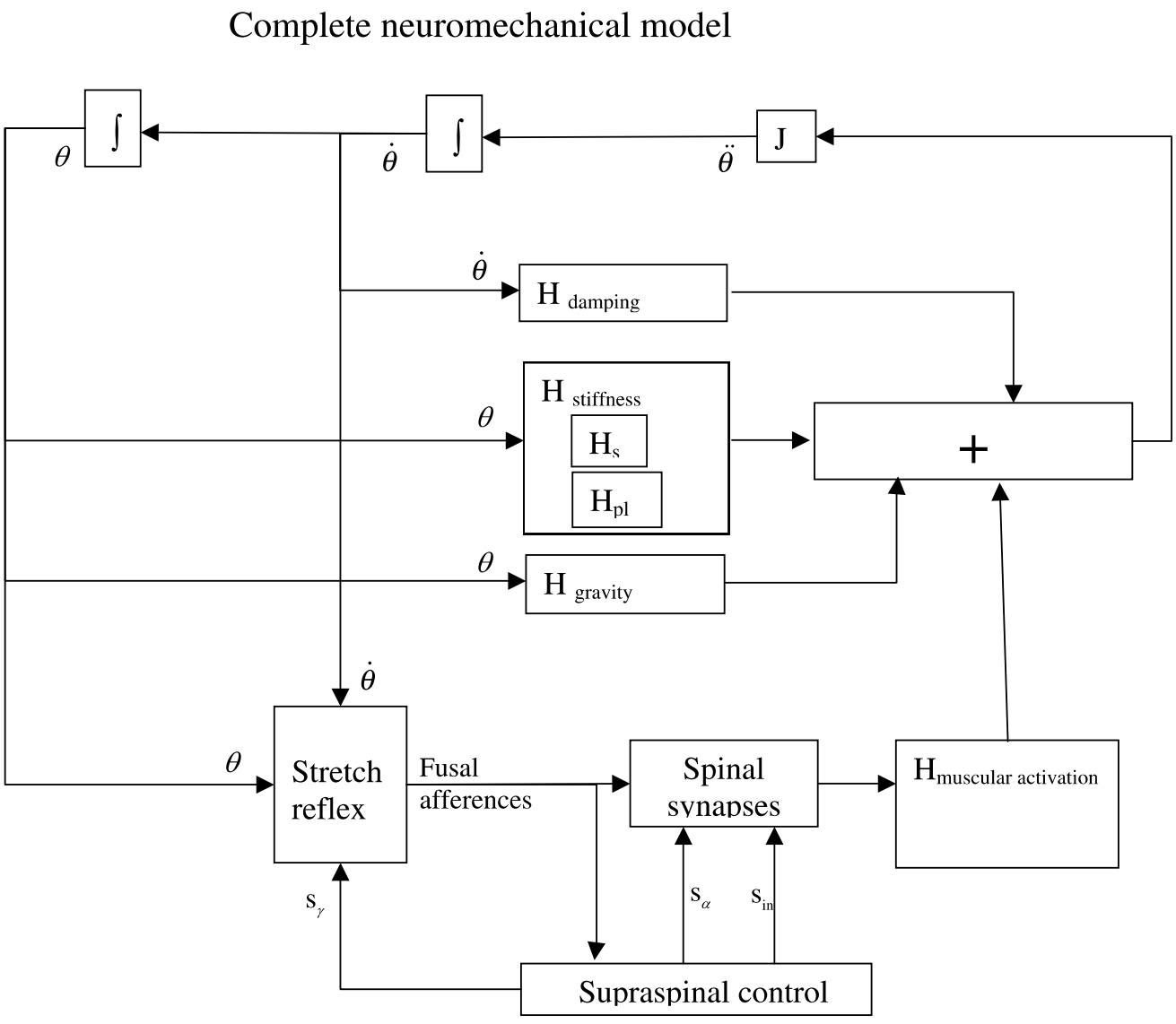

Fig. 2. Complete neuromechanical model. A complete description is given in Sect. 2

(gain G_p and exponential factor E_p), not available in the literature and thus identified by genetic algorithms:

$$H_{pl} = G_p e^{E_p \theta} . \quad (2)$$

This is an alternative to complex passive stiffness identification based on a particular experimental set-up, which does not lend itself easily to generalisation (Riener and Edrich 1999) or application to head movement (it is proposed in the literature only for limbs).

The second block (H_s) takes into account the linear part of the passive intrinsic stiffness characteristic, the so-called low stiffness:

$$H_s = K_s \theta , \quad (3)$$

where K_s is assumed to be equal to 0.5 N m/rad as for the head rotation (Zangemeister et al. 1981). These two blocks represent the passive intrinsic stiffness due to tissue characteristics. In the literature, it is often opposed to reflex-mediated stiffness (Sinkjaer and Magnussen 1994), which is included in our model in the stretch reflex block. There is another important effect on muscle stiffness – the active modulation, i.e. the stiffness increase due to voluntary muscle co-contraction. This is not included here, where we assume no co-contraction during the movement analysed. This hypothesis is supported by experimental observations of null EMG activation over the antagonist muscles during the fast inclination of the head used in our experiments (see appendix). In the case of further developments of the current model, this hypothesis should always be verified or the model should be modified properly.

2.2 Damping block ($H_{damping}$)

Another mechanical element considered is the damping ($H_{damping}$) of the systems involved in the movement:

muscles, connective tissues, ligaments and joints (Zangemeister et al. 1981). This contribution is modelled with a linear block depending on the head angular velocity:

$$H_{\text{damping}} = B\dot{\theta} \quad . \tag{4}$$

We have chosen to identify damping parameters (B) by genetic algorithms. Indeed, damping characteristics strongly differ between head rotation and head inclination because the different movement planes completely change the mechanical role of vertebrae and intervertebral disks. Hence, it does not seem appropriate to adopt the value proposed for head rotations in the work of Zangemeister et al. No other references were found in the literature for neck muscle damping values in frontal plane movements.

2.3 Gravity block (H_{gravity})

Since the head barycentre and the rotation centre are non-coincident, unlike head rotation in the coronal plane, the influence of the gravitational field (H_{gravity}) has been considered, as follows:

$$H_{\text{gravity}} = mgl\theta \quad . \tag{5}$$

In the range of head inclinations in the frontal plane, we approximate $\sin(\theta)$ with θ, which introduces an error below 3%.

In order to determine head barycentre [l in (5)], the volume of a 3D-head model has been projected on the frontal plane. The position of an average, approximated head rotation centre has been localised by studying the real movement geometry; it turned out to be 99.4 mm down the line connecting the zygomatic bones in the median position (see appendix for details).

2.4 Muscular torque generation

In the model, muscular torque is governed by an equivalent motoneuron activation input (s_α) (Hannaford and Stark 1985; Zangemeister et al. 1981). This signal acts directly on the $H_{\text{muscular activation}}$ block representing the voluntary force generation, whose function can be approximated by a 1-pole transfer function, as in (6):

$$H_{\text{muscular activation}} = \frac{G}{1 + ps} \quad . \tag{6}$$

The time constant (p in (6)) is 50 ms, the same as in Stark's works (Hannaford and Stark 1985) since the muscles involved in the investigated movements are the same (Kandel et al. 1994). The gain of this transfer function [G in (6)] was determined by traction experiments conducted on two normal voluntary subjects (average age 26), which provided a maximum moment generation of 3 N m (see appendix for details on this experimental activity). The alpha activation, s_α, which here represents the voluntary activation of alphamotoneurons, comes from the supraspinal control centres. s_α falls in the range $(-1, +1)$. Its signed value represents the difference of the activation of the two equivalent muscles, one right and one left equivalent muscle (Hatze 1981).

Actually the input of the muscular activation block is regulated by a spinal synapse block, which receives inputs from fusal afferences and the central nervous system (CNS) (s_α, s_γ and s_{in}) (Fig. 3). The way those inputs are composed strongly depends on the motor task. In physiology, the role of interneurons is very broad, modulating the stretch reflex on synergistic muscles, inhibiting the stretch reflex on antagonists and modulating the gain of stretch reflex depending on signals coming from the CNS, i.e. the motor task. In our work, we model the role of the interneurons such that s_{in} is the interneuron inibitory signal, which inhibits the stretch reflex during voluntary movements (as explained in detail in the following discussion). Actually, we model the complex mechanisms of inhibition and modulation of the stretch reflex due to supraspinal control (such as the stretch reflex of antagonist muscles and the presence of voluntary muscle activation).

In addition, there are fusal afferences which activate the stretch spinal reflex (Fig. 3). We assume here that their effect does not produce any contribution to muscular contraction during voluntary activation of muscles because of the counter-effect of the inhibitory interneurons (s_{in}) but governs muscular contraction through the stretch reflex mechanism when muscle length needs to be stabilised.

The stretch reflex (Kandel et al. 1994) originates from muscle spindles localised within the belly of postural muscles and run in parallel with the main muscle fibres. The value the CNS assigns to muscle length at the end of the movement depends on the sum of the facilitation and inhibition signals. Then, fusal afferences detect muscle length variations and trigger the spinal reflex: if length increases, they excite the motoneurons; if length decreases, they inhibit the motoneurons (and even excite antagonists). Thus, stretch reflex opposes muscle length variations, when a position is to be stabilised (Kandel et al. 1994). The stretch reflex has a double dependency, both static and dynamic, on the velocity and on the difference $\Delta\theta$ between the desired position (reference angle) and the actual position θ. This model well represents the two main afferent signals coming from spindles: group IA and group IIB. In addition, it includes a delay due to line transmission.

The block is thus composed of a function of head angular velocity (γ_{d}) and $\Delta\theta$ (γ_{s}) and a delay block, which takes into account the transmission delay (T_{r}). Two different solutions with respect to the definition of the delay were compared: a pure delay ($e^{-jsT_{\text{r}}}$) and a modification of the time constant of $H_{\text{muscular activation}}$. The chosen solution was pure delay, as expressed in (7), which best fits the curves and also best corresponds to physiology:

$$H_{\text{stretch reflex}} = (\gamma_{\text{s}}\Delta\theta + \gamma_{\text{d}}\dot{\theta})e^{-jsT_{\text{r}}} \quad . \tag{7}$$

The delay T_{r} (which corresponds to the monosynaptic reflex loop) can be estimated through a theoretical approximate calculation; a possible value for T_{r} should

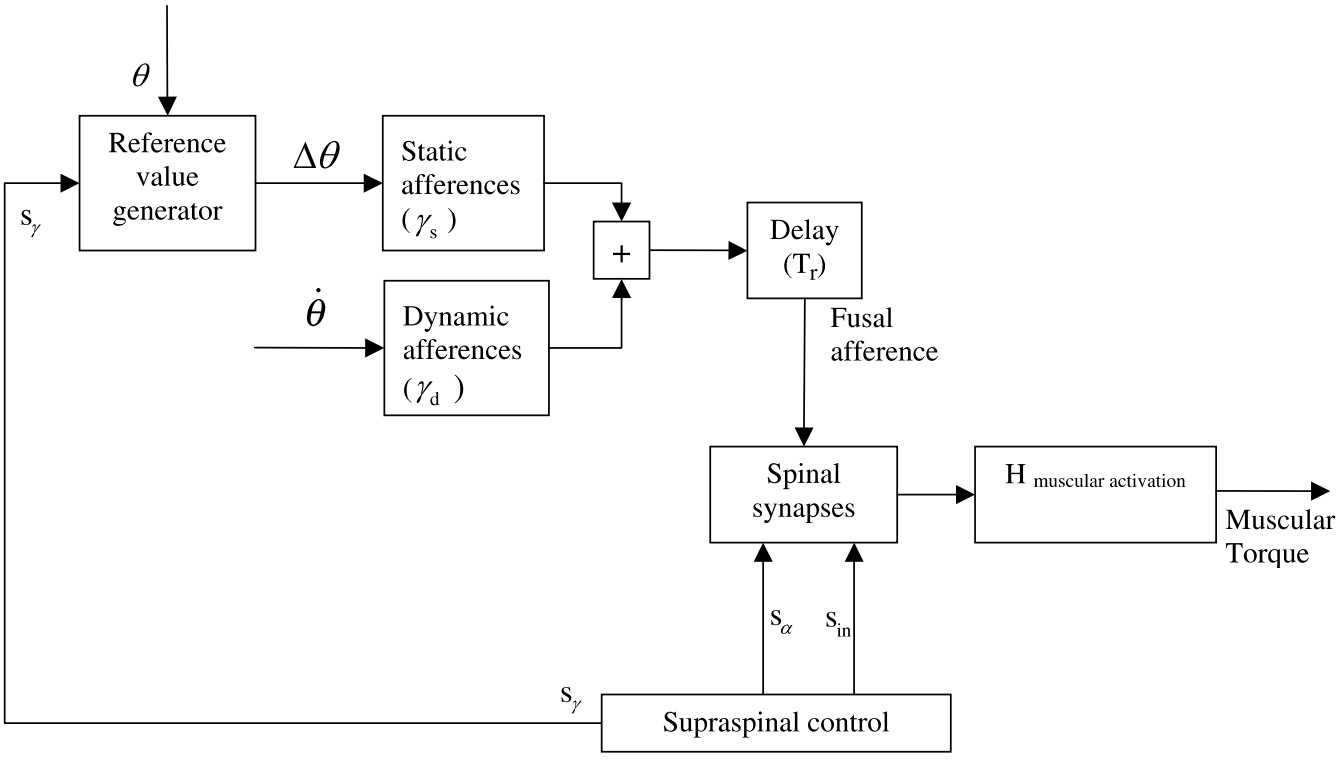

Fig. 3. Stretch reflex block diagram

range between 13 and 25 ms. Since it is a wide range and considering the numerous variations occurring in its definition, T_r will be identified together with the static gain γ_s and the dynamic gain γ_d by a genetic algorithm.

Vollbo et al. (1981) demonstrated that the fusal afferences are activated also during voluntary contraction and not only when position is to be stabilised. This is explained by the co-activation of intrafusal muscular fibres (gammamotoneuron activation s_γ) during alpha activation (s_α), which assures that the spindle in tension during muscle contraction will be maintained (Pearson and Gordon 2000).

The existence of alpha–gamma co-activation produces a contraction of the intrafusal fibres so as to adapt the reference angle during contraction, depending on the level of voluntary activation. In this sense, it is proposed that the stretch reflex may function as a servomechanism, that is, a feedback loop in which the output variable (actual muscle length) automatically follows a changing reference value (intended muscle length). In theory, this mechanism could permit the nervous system to produce a movement of a given distance without having to know in advance the actual load or weight bearing to be moved. In practice, however, the stretch reflex pathways do not exert sufficient influence over motor neurons to overcome large unexpected loads (Pearson and Gordon 2000).

Currently, the conditions under which independent activation of alpha and gamma motor neurons occurs in humans have not yet been established.

In our model, the servomechanism has been included only partially, i.e. gamma activation s_γ (co-activated by the supraspinal control with alpha) is present to adjust the reference angle during voluntary movement. s_γ is a control input to the reference value generator. However, unlike physiology, this servomechanism relies on the angle itself (θ from feedback line) instead of being modulated on the activation producing it (s_α); thus the possibility is excluded of using the stretch reflex as trajectory refinement to unexpected perturbation during movement, which is also rare in practice. Actually, the possibility of including this control will be proposed in the discussion, but it is not included in this work.

In order to define the reference value, a reference value generator is introduced (Fig. 3). It works like a θ-follower when s_γ is active and as a maintainer when s_γ is inactive. This way it is possible to memorise the position just when movement stops (the last frame with s_γ active), and this position is assumed to be the desired one to be stabilised until another voluntary movement is performed.

During voluntary contraction, afferences from spindles do not produce any muscular action, i.e. the stretch reflex is inhibited by interneurons (s_{in}), but are sent to the upper levels of CNS for high control of muscle length variations.

In conclusion, stretch reflex is included in our model as a stabilisation effect aimed at maintaining head inclination when no voluntary motion is required; this mechanism is able to work at any muscle length due to gamma activation. The gains (static and dynamic) of the stretch reflex are supposed to be fixed under the considered conditions and are identified by genetic algorithms as described in the discussion below; no references in the literature have been found to guess these values.

3 Methods

3.1 Experimental activity

In order to validate the model, head movements of seven voluntary subjects (average age 26) were acquired using an optoelectronic system for kinematics and electromyography acquisitions. For the kinematics data, we used four markers placed on right and left zygomatic bones and on right and left acromions, while for the electromyography we used four bipolar surface electrodes placed on sternocleidomastoids (right and left) and on trapezius (right and left). Three protocols were recorded: fast full-scale movements, fast movements with target angles, and stabilisation after small unpredictable perturbations. For the test related to target angles, a white inclined bar with a black background was projected in a dark room in front of the subject, who was asked to align his eyes with the bar as quickly as possible. The projected image was chosen randomly between a set of 24, 12 in a clockwise direction and 12 in a counterclockwise direction, obtained rotating the bar at 5° steps covering the range from 0° to 60°. Small unpredictable perturbations were produced by pulling, unexpectedly, a nylon wire fixed on one side of a helmet on the subject's head.

3.2 Identification algorithms

Genetic algorithms (GAs) have been used for the identification of the viscosity coefficient [B in (4)], the parameters of the H_{pl} block (2), the gains of the stretch reflex block (7) (γ_{s} and γ_{d}) and its delay (T_{r}). GAs fit particularly well in our optimisation problem because they do not require any particular regularity on the function, make use of a stochastic search method, avoiding the local minima problem, converge faster than other optimisation algorithms like Monte Carlo and can be easily adapted to the analysed problem (Davis 1991; Holland 1975).

The basic concept of GAs is the survival of a population of individuals. An individual is characterised by his genes, represented by the full set of parameters to be determined. Just as in nature the individual himself is the expression of his genes, in GA the genotype is represented by the unknown parameters and the phenotype is the output related to a particular genotype (fitness).

GAs manage a set of individuals for some generations. For each generation, every individual phenotype is evaluated and assigned a fitness value, which represents his adaptation to the environment. Once the GAs have evaluated the current generation, a new generation is created from the old one using a set of stochastic rules and applied to the fitness values of the previous generation, aimed at generating a set of individual candidates to survive. This process is executed until there is no fitness increment for a fixed number of generations or until a maximum number of generations is reached. The creation of the new generation is done in two steps:

1. Selection of the individuals from the old generation.
2. Implementation of the genetic operators to modify some of the selected individuals to create new individuals for the next generation.

For the selection process, a probability of survival is assigned to each individual, based on its fitness value. All individuals are listed by decreasing fitness. The first individual, with the highest fitness value, has a probability q of surviving to the next generation, while the i-th individual has a probability P_i of surviving according to the follow rule:

$$P_i = \frac{q * (1-q)^{n_i - 1}}{1 - (1-q)^N} \quad , \tag{8}$$

where N is the number of individuals in the generation, n_{i} is the position of the i-th individual in the list, q is the survival probability assigned to the best individual ($n_{\mathrm{i}} = 1$). The probability q is defined for the specific problem.

Each individual has an associated interval, with amplitude related to its survival probability P_i such that all individuals range in the interval between 0 and 1. When a random variable uniformly distributed from 0 to 1 is generated, a particular interval is selected, as well as the corresponding individual, which will take part in the new generation. Genetic operators are applied to selected individuals. There are two classes of genetic operators: recombination, which modifies the genotypes of two individuals, and mutation, which changes the genotype of the single individual. That is, implemented mutations are: uniform mutation, border mutation, non-uniform mutation and multiple non-uniform mutation. Recombinations used are: simple, arithmetic and heuristic. For a detailed description of each genetic operator see Michalewicz (1994).

Once the selection of survived individuals is performed, half of the individuals of the population are modified by genetic operators; some differences in this criterion are implemented in the different phases of the study and will be discussed in the following discussion below. The choice of the individuals to be modified is random, keeping the same probability of application for all the operators. Regarding the termination criteria, different solutions are adopted and will be discussed for each phase of the work.

4 Model identification

The identification process was divided into two steps: in the first, H_{damping} and H_{pl} [the parameters: B in (4); E_{p}, G_{p} in (2)] have been identified; in the second, the stretch reflex block parameters [T_{r}, γ_{s} and γ_{d} in (7)] were computed. The raising phase of fast full-scale movements was used to identify the H_{damping} and H_{pl}; hence, during the raising phase of such fast movements, the stretch reflex contribution was assumed to be inhibited by interneuron s_{in}, thus leaving s_α as the only input to muscular activation. This hypothesis is supported by the analysis of the electromyography data. The EMG, recorded for the fast full-scale movements, showed only a very high activation of homolateral muscles during the whole raising phase of the movement (see appendix for details).

On the other hand, the movements after small unpredictable perturbations were used for the identification of the structure and of optimal values of the stretch reflex block parameters. The movements were small and unpredictable, and the absence of voluntary force generation was hypothesized, i.e. s_α and s_{in} can be considered null, and thus the return to the equilibrium position only relies on the stretch reflex.

4.1 Determination of the $H_{damping}$ and H_{pl} blocks

For the identification process we used 85 out of 153 fast full-scale movements acquired on all seven subjects, limiting the analysis to only the raising phase, as previously discussed. The choice to use only part (about 60%) of the recorded curves is necessary to build a testing database (not used in the identification to avoid biases), used to verify the generalisation ability of the model. Movement onset was defined on the leading edge of angular velocity at 0.05 rad/s; movement ends on the trailing edge, when velocity returns equal to 0.05 rad/s.

To synchronise and normalise the curves, they were rescaled in time and amplitude. From such processed data the mean curve and its standard deviation were calculated. The assumption of this phase of the identification (related to the type of movement: raising phase of fast full-scale inclination) is that s_{in} is activated so as to cancel the contribution of the stretch reflex opposed to the voluntary motor activation; hence the only input to $H_{\text{muscular activation}}$ is s_α. Anyway, s_γ is coactivated with s_α; thus the reference value generator works as a follower (servomechanism of the stretch reflex presented in the model description section).

The input s_α was estimated from considerations on EMG traces: we processed the EMGs recorded for fast full-scale movements and computed a reference trace (see appendix). This reference was assumed to be equal to the contribution of the muscular force in the model, i.e. the output of $H_{\text{muscular activation}}$.

Hence the corresponding s_α was estimated with a normalised three-rectangle pattern (rect1: amplitude 1, duration 0.14 s; rect2: amplitude 0.5, duration up to 0.30 s ($\Delta t = 0.16$ s); rect3: amplitude 0.22, duration up to 0.52 s ($\Delta t = 0.22$ s)).

The fitness η_j for the j-th individual (i.e. the j-th triplet of possible solutions) was defined as

$$\eta_i = \frac{\sum^N i\, d(cj(i); m(i))}{\text{std}(i)} \quad , \tag{9}$$

where N is the number of samples, $c\,j(i)$ is the i-th sample of the j-th output curve corresponding to the j-th individual, $m(i)$ is the i-th sample of the mean curve calculated from the experimental data and std(i) is the i-th sample of the standard deviation determined by the experimental data. d(,) is the distance function. The genotype of the j-th individual is defined by the triplet ($B\,j$, $G_p\,j$, $E_p\,j$), which corresponds to a phenotype represented by the cj curve.

To fix the number of individuals for each generation and the number of generations needed before the GA ended, a preliminary study was done. We fixed the number of individuals at 50 and studied the results of 20 independent GAs evolving for 200 generations. The fitness improved very fast during the first 30 generations and continued to increase slowly after that. This suggested that the GA was stabilised only after a large number of generations and did not guarantee that the absolute minimum would be reached. To solve this problem, we chose a hybrid implementation: we calculated more independent GAs, each one composed of 50 individuals, let them evolve for 100 generations, and then plotted the distribution of the best individuals determined from each GA (one individual for each GA), visualising the fitness in the search space. Very broad parameter ranges were initially defined; successive restrictions focused the analysis on the basis of previous cycles' results until the the optimum value for the unknown parameters was determined. In this way we determined the minimum and maximum edges for the parameters. With the last cycle we determined the optimum value for the unknown parameters: $G_p = 79.432$ N m/rad, $E_p = 5.394$, $B = 1.707$ N m s/rad, which is equivalent to a fitness of 3.152, corresponding to a mean error for each sample of 2.9% with respect to the mean real data curve.

4.2 Determination of the stretch reflex parameters (γ_s, γ_d and T_r)

Once the damping and physiological limit blocks were determined, we proceeded with the second step of the identification process, keeping the defined mechanical contribution fixed. In this phase, the hypothesis that there is no voluntary movement activation, i.e. s_α is null, as well as s_{in} and s_γ, has been stated. Under this assumption, the only mechanism activating the muscles is the stretch reflex. This is assumed true since we considered the first reaction to small and unpredictable perturbations to the head position.

Under this configuration the unknown parameters of the model are γ_s, γ_d and T_r, as defined in (7).

To build the mean curve needed for the identification process, we considered the data recorded for stabilisation movement after a small external unpredictable perturbation. The curves were translated to have all final angles equal to zero, representing the occurred stabilisation. We considered the data only from the first minimum after the first fast return phase to the end of the movement.

We implemented GAs similarly to the first identification phase, i.e. a hybrid solution, using the same fitness η. The search space for the unknown parameters was fixed by a preliminary consideration: for γ_s and γ_d we tested only the value for which the output moment was of the same order of the voluntary moment, while a T_r range of 13–25 ms was imposed, as was expected by physiological considerations.

The optimal identified values are: $\gamma_s = 8.33$ N m/rad, $\gamma_d = 0.568$ N m sec/rad and $T_r = 0.014$ s, which correspond to a fitness of 0.069 equal to a mean error of 0.15% for each sample with respect to the mean curve of real data.

Table 1. Identified model parameter values

	Equation	Parameter	Value	Origin
$H_{\text{stiffness}}$ (H_s)	(3)	K_s	0.5 N m/rad	Zangemeister et al. (1981)
$H_{\text{stiffness}}$ (H_{pl})	(2)	G_p	79.432 N m/rad	GA
		E_p	5.394	GA
H_{damping}	(4)	B	1.707 N m s/rad	GA
$H_{\text{stretch reflex}}$	(7)	γ_s	8.33 N m/rad	GA
		γ_d	0.568 N m s/rad	GA
		T_r	0.014 s	GA
$H_{\text{muscular activation}}$	(6)	G	2.96 N m	Experiments (see appendix)
		p	0.05 s	Zangemeister et al. (1981)
H_{gravity}	(5)	m	4.9 kg	Anthropometrical tables
		l	12.8 cm	Experiments (see appendix)

4.3 Model implementation

In Table 1, the values of all the parameters used in the model are reported. The model is implemented in Matlab Simulink 6.1.

5 Model validation

5.1 Model validation for fast full-scale movements

The identification process lets us determine the optimal value for all the unknown parameters of the model for the two phases of the considered movement. To validate the found values, we compared the complete model output with the 153 fast full-scale curves acquired by the ELITE system.

In order to make a consistent comparison, all the curves were resized so that they had an initial angle equal to zero, and we cut them so that they had a duration of 1.5 s until stabilisation. For this validation phase the same s_α signal, derived by EMG as in the first phase of the identification, was used. Sg was co-activated with s_α, and s_α was assumed to inhibit the stretch reflex during alpha activation and then, being inactive, allowed the stretch reflex mechanism (fusal afferences) to activate the muscle. A very good fitness of the model over the fast full-scale movements (including the stabilisation phase) is quantitatively confirmed by the square correlation coefficient ($r^2 = 0.955 \pm 0.053$, $N = 153$); some examples are given in Fig. 4.

Model validation for fast full-scale movements is confirmed also by the analysis of two more parameters: the time to reach the maximum angle and the absolute value of the maximum reached angle. The model presents a mean time to reach the maximum angle equal to 0.24 s, while the median value calculated from the experimental data set is 0.28 s and mean value is 0.31 s. Regarding the maximum reached angle the model shows a mean output equal to 34°, while the mean value from experimental data is 33.8°.

The robustness of the identified model is hence supported both by the use of all 153 curves (only 85 were used for identifying the parameters) and by the use of the whole curve (raising + stabilisation). Indeed, the identification process was split into two separate phases for the identification of the parameters relative to the first and second raising phases for the identification of the stretch reflex parameters.

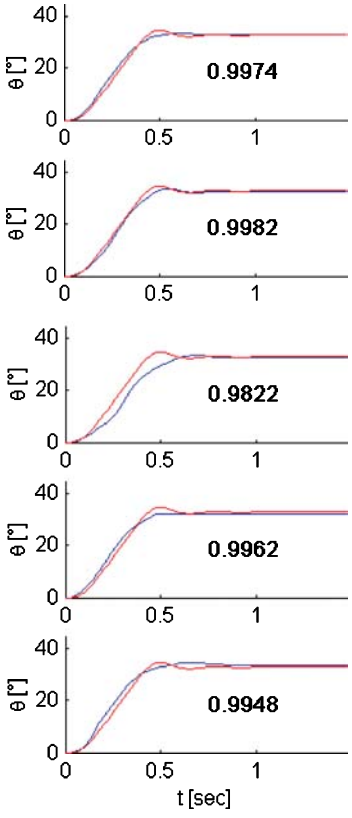

Fig. 4. Examples of experimental curves and correlation coefficient (*blue* experimental data, *red* model output). The curves shown here belong to testing data (not used for identification). Model output well reproduces experimental trials, as confirmed by correlation coefficients. The difference between model behaviour and each trial is within experimental data variability

5.2 Model generalisation

To generalise the model validity, its ability to represent medium-scale range movements has also been studied. For

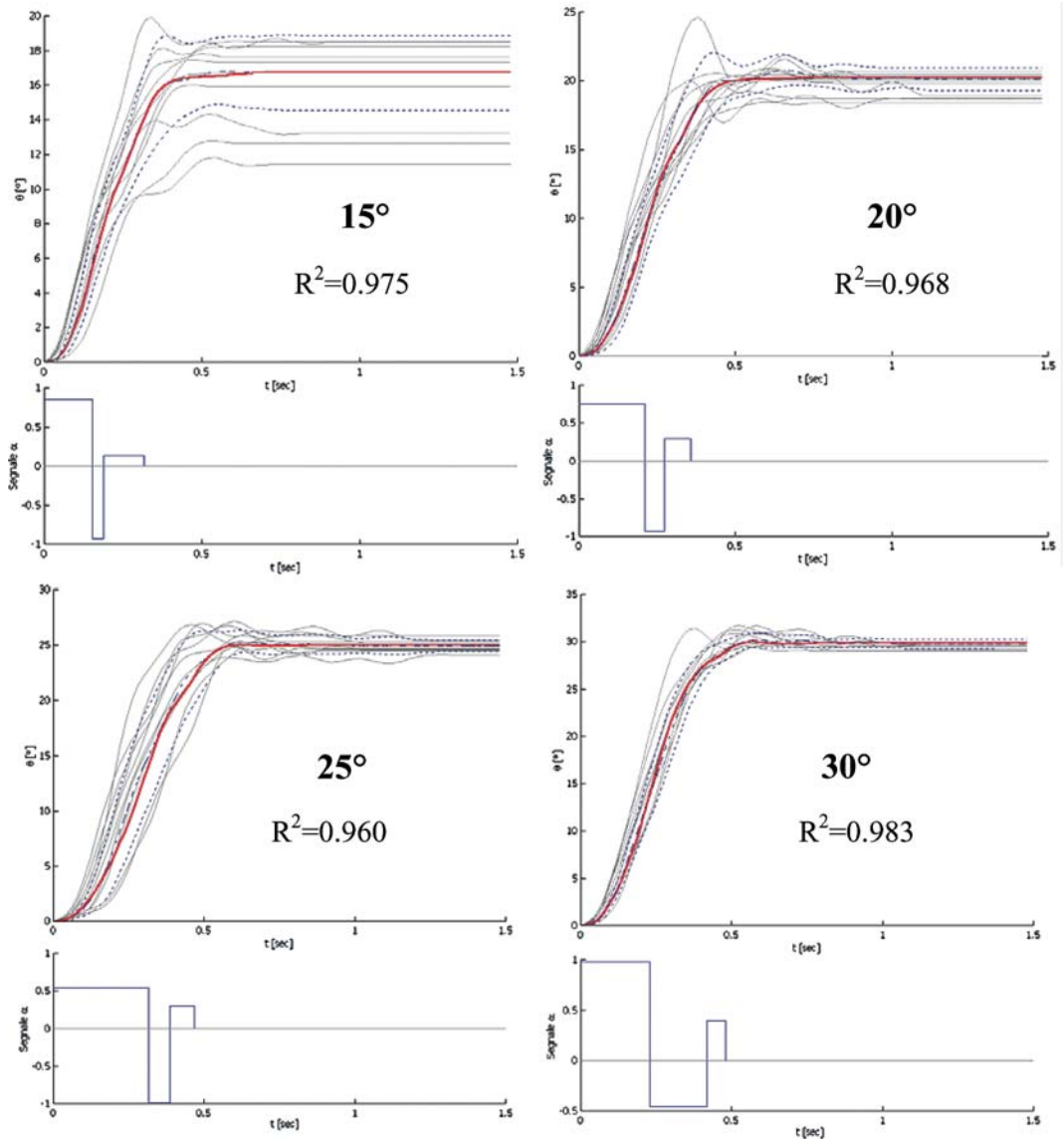

Fig. 5. Target angle results: 15°, 20°, 25°, 30°. The *upper panels* give the kinematics data used for validation and the simulated curves (*red thickest*) along with the average correlation coefficient between the model output and the recorded curves. The *lower panels* show the correspondent triphasic input signals identified by GA for each target angle

this purpose, the data for fast movements toward a target angle were considered. In this case we needed to determine the voluntary signal s_α for the model. The curves were divided into four groups, clustering the ten curves that had a final angle closest to 15°, 20°, 25° and 30°, and for each group the mean curve was calculated (Fig. 5).

Again, under these configurations it was assumed that the s_{in} deactivated the stretch reflex when s_α was not zero, and s_γ co-activated with s_α. On the other hand, when s_α was zero, s_γ and s_{in} were zero, too, and the fusal afferences were the unique input to $H_{\text{muscle activation}}$ representing the stretch reflex.

To determine the optimal input signal s_α for each group of curves, a genetic approach was used. It was assumed that s_α was constituted by three adjacent rectangles because of the study made on the EMG and of the results in the literature (Kandel et al. 1994). Since six parameters are to be determined (duration and amplitude of each rectangle), GAs were adopted in a six-dimensional space. In this s_α identification process, we chose to use the same η fitness and a hybrid implementation of GAs that we used previously. Because of the six-dimensional research space, it is worthwhile to use a large number of individuals. We chose to have a population of 500 individuals, but this choice implied an increase of computational time. To face this problem, we required the GA to finish if there was no improvement in the fitness for more than ten consecutive generations. To maintain a high dynamic and to limit the effects of a possible premature termination, a large number of individuals was involved in the process of genetic modification; in particular 266 individuals for each generation were modified and equally distributed between the genetic operators. For each group of curves, 80 GAs were calculated. The GAs determined a triphasic s_α

for each group (Fig. 5). Time-amplitude characteristics were in agreement with the results in the literature (see, for example, Hannaford and Stark 1985). Moreover, the morphological comparison between the target angle data and the output curves generated using the identified s_α showed great correlation, as shown in Fig. 5.

5.3 Complete model performance

To test the behaviour of the model in the whole range of inclinations in the frontal plane, the four identified s_α have been interpolated to build the input signals for angles in the whole range (15–30°). For every 2° angle in this range, we used the corresponding interpolated s_α as model input and compared the theoretical angle to the one reached by the model. It was found that the model generated an output curve whose final angle was very close to the theoretical angle (Table 2).

6 Discussion and conclusions

The aim of this paper was to determine a model for fast head movements in the frontal plane, which includes the main anatomic and physiological aspect of the head–neck joint control, because of its intrinsic relation with the alignment of the infra-orbital line with the horizontal plane. The first part of the paper was devoted to the identification of the principal contributions to head movement and of the relations between them. Thus, in parallel with the voluntary force generation, we considered the contribution of gravity field, damping, tissue stiffness, physiological limits imposed on the movement by anatomical constraints and stretch reflex. Some of the relevant parameters were derived from the literature (namely, when we could extend the results of Stark and his workgroup's model about head rotation on the coronal plane). In particular, we adopted the dynamics of the voluntary moment generation (for the gain we used experimental traction tests; see appendix) and the low stiffness coefficient proposed, while we discarded the damping coefficient because the characteristics of the tissues in the two movements are strongly different. Furthermore, we introduced new blocks representing the physiological limits, the gravity field and, most of all, the effect of the stretch reflex.

Finally, the structure of the stretch reflex block was thought to take into account some physiological evidences such as its dependency on the relative position ($\Delta\theta$) and angular velocity and the delay due to the line transmission (7). Spinal synapses activity was modelled according to physiological considerations, taking into account basically two mechanisms: the co-activation of alpha (s_α) and gamma (s_γ) efferences and the presence of interneuron inhibition (s_{in}) of the stretch reflex during voluntary contraction (when s_α is active).

The model determined in this way presented six unknown parameters: the damping coefficient B, the gain G_{p} and exponent E_{p} for physiologic limit block, the static γ_{s} and dynamic γ_{d} gain and the delay T_{r} for the stretch reflex block (reported in Table 1).

The identified values of those parameters can hardly be compared to other works in the literature. In the case of the damping coefficient [B in (4)], we found a value which is one order of magnitude different from the one proposed by Stark et al. for head rotation (in the horiziontal plane). Actually, this could be due to the fact that a completely different role is played in the two movements by the vertebrae and the intervertebral disks. The physiological limit block parameters (2) reproduce well the expected sharp exponential curve, which is also found by experimental data for limbs' elastic property identification (Riener and Edrich 1999). In this framework, it is worth noting the simplicity of the experimental set-up used in our case, especially considering that head motion was the movement studied.

Regarding the stretch reflex block identification, as far as we know, many studies are available which model the fusal afferences and investigate the physiology of the modulation of those afferences, but much less is available in the literature on the stretch reflex gain modulation. Actually, except for the good performance of the model in our experimental validation, we did not find similar models in the literature to compare the γ_{s} and γ_{d} values (7). On the contrary, the value found for the stretch reflex delay [T_{r} in (7)] definitely corresponds well to the approximate calculation based on the length and velocity of the monosynaptic reflex.

For the identification of the optimal values for these parameters, two different protocols were adopted: fast full-scale movements and stabilisation after a small and unpredictable perturbation. The data were acquired using ELITE and the numerical identification was performed by GAs.

The successive verifications of model validity and ability to generalise showed the good performance of the whole model. The comparison between the output curve of the model with the fast full-scale data confirmed how the identified model is representative of the fast full-scale real voluntary movements. In addition, it has been demonstrated that the model is a useful instrument for representing the whole range of fast head inclination in the frontal plane. In fact, the results of the identifications for the optimal s_α for target angles are in complete agreement with other studies and experimental data in the literature. This characteristic is proved also by the behaviour of the model in response to an input signal obtained by interpolation of the identified ones. Using an interpolated signal

Table 2. Percent error over the whole range of inclinations of the model output using interpolated inputs

Desired angle (°)	Error (%)
17	−0.64
19	−0.93
21	−0.44
23	1.34
24	−0.30
26	0.41
28	0.67

relative to a desired angle (see section on model generalisation) the model generated curves with final angles very close to the desired ones over the whole range of possible inclinations in the frontal plane.

Three strong hypotheses have been assumed for the definition of the current model. First is the linear summation of the neural inputs. This hypothesis will be discussed on the basis of future investigations adopting the model in specific protocol set-ups; it is not explicitly exploited for the current neuro-muscular model. Second is the absence of active stiffness modulation due to co-contraction. This assumption is strongly related to the choice of modelling only fast movements where we assume only two contributions to stiffness: the passive stiffness (represented by the low stiffness block and the physiological limit block) and reflex-mediated stiffness (due to the stretch reflex). The third stiffness contribution usually discussed in the literature (see for example Sinkjaer and Magnussen 1994) is the one determined by voluntary co-contraction; this latter has been neglected here because EMG recorded tracings supported the hypothesis that no voluntary co-contraction was relevantly observed in the types of movement studied (see appendix). Future applications of the model to different movements will need to consider such a contribution.

The third hypothesis relates to the function of the spinal synapses, which produce alpha and gamma co-activation and the activity of interneurons (s_{in}), which inhibit the stretch reflex during voluntary contraction. In this way, during voluntary contraction fusal afferences (which are modulated on the servomechanisms, thus updating the reference length value, due to s_γ activation) are only going to supraspinal centres and are not used for trajectory refinement. Actually, the use of the stretch reflex for trajectory refinement during voluntary movements has been proposed by physiologists when small unexpected loads occur, but in practice, the contribution of the stretch reflex is rarely able to perform the correction (Kandel et al. 1994). This simplifying assumption is necessary because we modelled the reference angle calculated from the feedback line (Fig. 3) and not directly coming from supraspinal control and in addition because we completely inhibit the stretch reflex during contraction. Actually, it could be possible to modify the model to include this effect. We can assume that a noise on the total torque is included which accounts for unexpected small perturbations. On the other hand, we may assume the existence of a complete reproduction of the model without noise in the supraspinal control, a sort of efference copy (it should be in the cerebellum). This efference copy could be used to generate the reference value coming with gamma activation. Thus, the reference value corresponds to a required desired angle, coming from CNS, and is compared with the actual value coming from an actual feedback line (where the noise could have introduced a disturbance in movement trajectory). Hence, the fusal afferences can measure this noise and the stretch reflex can produce a muscular activation so as to correct the irregularity provoked by the unexpected perturbation. In this way, the inhibitory interneurons should be used accordingly to modulate the gain of the stretch reflex.

In conclusion, in this work we have built a model for head–neck segment fast movements in the frontal plane, which, with respect to the principal anatomical and physiological aspects, represents, under few assumptions, the neuro-mechanical response to an equivalent neuronal input signal. It could provide a useful tool for investigating how the various sensorial systems contribute to the modulation of the alpha activation.

Furthermore, the use of GAs in this field seems to be very promising with respect to classical parameter identification of muscle models which are often based on very complex experimental set-ups. From this perspective, it is worth discussing the usability of such a methodology for biomechanical modelling in general. Usually, limb modelling uses a composition of models, one for each muscle acting at the considered joint. This approach can apply to different movements of the same joint but requires very complex and not as reliable measures of each muscle's parameters. Those parameters, used especially to define the force length/velocity curves, are usually identified either by dedicated experiments, where the contribution of the single muscle is hardly separated by its agonist muscles, or by measures on cadavers. Our approach is much more reliable when co-activation of agonist muscles is present and is very simple to apply when the tissues participating in the production of joint movement are complex. Furthermore, the experiments required for identification are very simple. On the other hand, our model is very movement dependent because the parameters' values are applicable only to the joint movement which was used to identify them (for example only in the frontal plane and at high velocity). In addition, we have parameters which describe all the effects and we are unable to separate the contributions of the different tissues and muscles.

So far, our model is completely time invariant, and no modelling of fatigue is included. In principle, it could be added to muscular activation modelling by modulating the maximal moment exertable, but dedicated experiments would be required for evaluating the impact of fatigue.

Acknowledgements. The authors wish to thank Prof. L. Stark and Prof. V.V. Krishnan for the precious brainstorming and Mr. Eng. M. Locati and Eng. A. Lentini for the conduction of experiments, contributions to GA algorithm development and data processing.

References

Amblard B, Assaiante C, Fabre J-C, Mouchnino, Massion J (1997) Voluntary head stabilization in space during oscillatory trunk movements in the frontal plane performed in weightlessness. Exp Brain Res 114:214–225

Barberini CL, Macpherson JM (1998) Effect of head position on postural orientation and equilibrium. Exp Brain Res 122: 175–184

Basmajian JV, Clifford HC, McLeod WD, Nunnalay HN (1975) Computers in electromyography. Butterworths, London

Berthoz B, Pozzo T (1988) Intermittent head stabilization during postural and locomotory tasks in humans. In: Amblard B, Berthoz A, Clarac F (eds) Posture and gait: development, adaptation and modulation, Elsevier, Amsterdam, pp 189–198
Bronstein AM (1988) Evidence for a vestibular input contributing to dynamic head stabilization in man. Acta Otolaryngol (Stockholm) 105:1–6
Davis L (1991) Handbook of genetic algorithms. Van Nostrand Reinhold, New York
Guitton D, Kearney RE, Wereley N, Peterson BW (1986) Visual, vestibular and voluntary contributions to human head stabilization. Exp Brain Res 64:59–69
Hannaford B, Stark L (1985) Roles of the elements of the triphasic control signal. Exp Neurol 90:619–634
Hatze H (1981) Myocybernetic control models of skeletal muscle: characteristic and applications. University of South Africa, Pretoria
Holland JH (1975) Adaptation in natural and artificial systems. MIT Press, Cambridge, MA
Kandel ER, Scwartz JH, Jessell TM (1994) Principi di Neuroscienze, 2° edizione, ed. Ambrosiana
Pearson K, Gordon J (2000) Spinal reflexes. In: Kandel ER, Shwartz JH, Jessel TM (eds) Principles of neural science, chap 36. McGraw-Hill, New York pp 713–736
Pedotti A, Ferrigno G (1985) ELITE: a digital dedicated hardware system for movement analysis via real-time TV signal processing. IEEE Trans Biomed Eng BME 32:943–950
Pozzo T, Berthoz A, Lefort L (1990) Head stabilization during various locomotor tasks in humans: I. Normal subjects. Exp Brain Res 82:97–106
Pozzo T, Berthoz A, Lefort L, Vitte E (1991) Head stabilization during various locomotor tasks in humans: II. Patients with bilateral peripheral vestibular deficits. Exp Brain Res 85: 208–217
Riener R, Edrich T (1999) Identification of passive elastic joint moments in the lower extremities. J Biomech 32:539–544
Sinkjaer T, Magnussen I (1994) Passive, intrinsic and reflex-mediated stiffness in the ankle extensors of hemiparetic patients. Brain 117(2):355–63
Zangemeister WH, Lehman S, Stark L (1981) Simulation of head movement trajectories: model and fit to main sequence. Biol Cybern 41:19–32

Appendix

EMG data processing and results

Data processing The EMG signal was recorded by bipolar electrodes placed on left and right sternoicleidomastoids and left and right trapezes. A band-pass pre-filter (10–200 Hz) was applied, and the signal was then rectified and lowpass filtered with a transition band from 5 Hz (max. attenuation 0.3 dB) to 10 Hz (min. attenuation 3 dB) (Basmajian et al. 1975).

A threshold defining the EMG activation level was determined on the basis of the mean value and standard deviation of the activation recorded during initial posture (baseline EMG). The threshold (for each muscle) was fixed when EMG tracing overcame the double of the standard deviation of the baseline. No activation of the antagonist muscles was ever observed during the raising phase of the fast full-scale movements.

Calculation of reference EMG A reference EMG has been used to determine the input voluntary activation for the raising phase of the fast full-scale curves (ballistic movements of the head). Twenty-eight EMG traces were used for the estimation of the reference EMG. EMG traces were subtracted by the baseline and normalised by their maximum values in order to compensate possible asymmetries of electrodes positioning and different muscle characteristics.

To estimate the reference EMG, we used the average EMG. The input signal s_α used was composed of three rectagular stimuli (Stark et al. 1985):

- rect 1: Amplitude 1 duration 0.14 s.
- rect 2: Amplitude 0.5 duration 0.16 s.
- rect 3: Amplitude 0.22 duration 0.22 s.

To validate the identified s_α, the reference EMG has been compared to the output of the $H_{\text{muscular activation}}$ produced.

Head geometrical and inertial parameter estimation

Head barycentre In order to estimate the position of the barycentre of the head, we performed a study on a geometrical and analytical three-dimensional model. The model was designed to reproduce normal human head proportions and scaled on subjects' sizes. Then, we made 101 slides of the model in the horizontal plane. Projecting the slides in the frontal plane we built a head map M, where all the point values were proportional to the thickness of the head at that level. We scaled the values of this map so as to reach a total head mass equal to 4.9 kg (derived from anthropometrical tables for a man weighing 70 kg). In this way we calculated the discrete distribution of mass and then the static components of the static moments followed by the position of the barycentre, divided by the head total mass. The head barycentre resulted at 28.6 mm above link between the zygomatic bones.

Barycentral inertial moment of the head By using the same map M defined for the head barycentre estimation, the inertial moment of the head was calculated, leading to a value of $J_g = 0.025\ \text{kg m}^2$, which is slightly bigger than the one used by Stark and colleagues, who assumed the head to be a sphere filled with water.

Head rotational axis We used inclination movements of the head to estimate the head rotational centre in the frontal plane. Data were low-pass filtered to reduce error. The head rotation centre was determined to be 99.4 mm away from the link between the zygomatic bones at its midline. Hence, the distance between the head barycentre and the head rotational centre [l in (6)] is 12.8 cm.

Maximal moment experimental estimation

To estimate the maximal moment generated by the head inclination, i.e. the gain of the $H_{\text{muscular activation}}$ block, experiments were performed on three subjects. The subjects sat with head horizontal and asked to align their head with the vertical plane, keeping the shoulder fixed (they were firmly fixed to a support). A thread was fixed to a helmet worn by the subjects, and the thread was aligned with the horizontal plane of the head barycentre by a vertical support (without friction). Different loads (from 0.5, 1, 1.5, 1.8, 2, 2.3, 2.5 and 3 kg) were attached at the thread extremity. The thread was long enough to be in tension with the loads still on the floor. The subjects were asked to move the head as fast as possible to bear the load. Ten trials for each side and for each subject were executed. The maximal load raised was 2 kg. By geometrical considerations, the moment arm was calculated (depending on the head inclination, which was acquired with the ELITE system, as with the other experimental activities). The corresponding maximal moment exerted by the head turned out to be 2.96 N m, which has been approximated to 3 N m in the $H_{\text{muscular activation}}$ block.